RELIABILITY ASSESSMENT AND PERFORMANCE ANALYSIS OF HYBRID CONTROLLERS USED IN ELECTRIC VEHICLE APPLICATION

Raghavaiah KATURI[1], Srinivasarao GORANTLA[2]

Smooth transition of battery and ultracapacitor (UC) is the main difficulty associated with multiple energy storage structures (MESS) powered electric vehicles (EVs). The main objective of this work is to design a novel control strategy, which will make a smooth transition of energy source in MESS corresponding to the vehicle requirement. A new controller is considered with four individual math functions related to the various speed conditions of the motor titled as a condition-based controller (CBC). Thereafter, the considered CBC is combined with various controllers in order to achieve the main objective of the work. In this, the designed CBC controller is combined mainly with four other controllers named proportional-integral (PI), proportional integral derivative (PID), the fuzzy logic controller (FLC) and artificial neural network (ANN) formed four separate hybrid controllers. All controllers' performance is mainly examined in four cases at different load conditions. In this work, the solar system is adopted to charge the battery during sunlight and irradiance available timings. Finally, a comparative analysis is done among all controller's performance by considering various time domain specifications.

Keywords: DC-DC converters, PI controller, PID controller, fuzzy logic controller, ANN controller, CBC.

1. Introduction

Many of the researchers are mostly concentrated on developing an eco-friendly transportation system because the conventional transportation system creating much pollution in the atmosphere. Electric vehicles are developed after serval decades to reduce the pollution that might be air or sound pollution. Conventionally majority of EVs are power with battery and which will have some drawbacks like driving range as well as low power density. Thereafter MESS based electric vehicle to avoid some of the draws associated with conventional EVs. The MESS was developed by combining the battery with UC; here UC doesn't have high energy density so it could not use for continuous power supply to the load. To obtain the proper power-splitting of two energy sources according to the electric vehicle requirement several conventional as well as intelligent

[1] Research scholar, Dept. of Electrical Engineering, VFSTR Deemed to be University, India, e-mail: raghava.katuri@gmail.com

[2] Prof., Dept. of Electrical Engineering, VFSTR Deemed to be University, India.

controllers developed. Proper power splitting of MESS during real-time implementation is the major challenge associated with electric vehicles. A rule-based energy management strategy has been proposed to obtain the optimized energy sharing of the battery and UC also considered the dc-dc converter with less switching losses [1]. EV is designed with solar power-assisted battery, which indicates that the battery of the EV gets charged from the solar power. In solar balancing case battery gets charged from solar power, in storage balancing case battery charged from conventional power storage at that time of stoppage of a vehicle and in charge balancing case battery can discharge the power to the load [2]. Generally, for implementing solar to vehicle charging strategy integration is one of the difficult factors related to EVs. Swapping of the batteries from battery stations to the vehicle can be done for vehicle propulsion. Battery storage systems are runs with solar power as well as conventional power, to develop the independence of EVs self-charge mechanism was developed with solar which is inbuilt integrated into the vehicle. With this arrangement battery of the EV can charge from the vehicle panel during sunlight available time [3]. Asymmetric bidirectional Z-source topology was proposed for MESS based EVs for proper power balancing between battery and UC. With the developed topology maximum utilization of UC can be achieved [4].

Optimal allocations of the solar plants benefit the economy of the industry. This optimal allocation is also a very difficult factor due to the continuous changing condition of utilization as well as the availability of sunlight [5]. Due to low kinetic dynamics of the vehicle battery internal resistance can be increased this cause to the reduction of the capacity of the source; to overcome this MESS is introduced with different practical cases [6]. For improving the life of the battery superconducting magnetic energy storage was considered and combined, made MESS. The designed MESS system enhances the electric bus performance by increasing the life of the battery and dismissing the size of the storage system [7].

Two different real-time controllers are developed to share the power to battery and UC which will use to protect the state of health of the battery. Based on Karush–Kuhn–Tucker conditions one controller is designed and another one is designed based on the neural network. Further developed two controllers are implemented in real-time to the electric vehicle [8]. For a specific electric vehicle point of view, MESS is introduced by combining the battery with a supercapacitor and smart energy as well as power-sharing can be achieved by the fuzzy logic control system [9]. Electric vehicle charging stations are one of the major issues with well-developed countries. Generally, all-electric vehicles are charged from the local plug-in charging stations which will create an extra burden on the power grid, which means they're an internal deficiency that occurs in the distribution system. To avoid that situation PV based power generation is incorporated with the electric vehicle itself and utilized the power whenever the sunlight is available. If sunlight is not available then the electric vehicle can be charged from the conventional grid, all this can be achieved with an optimized algorithm [10]. In MESS powered electric vehicles smart energy management is one of the major challenges. Particle swarm optimization incorporating the Nelder–Mead simplex technique is proposed to make the possibility of smart energy management between the battery and UC [11].

A nonlinear case predictive control was developed for splitting the energy between supercapacitor and battery. Furthermost of the countries in the world are focused on emerging an electric vehicle which will create an extra burden on the local substations. Solar power stations are developed along with conventional grids and the photovoltaic (PV) system also included within the vehicle itself for a better driving range of the electric vehicle [12].

The main scope of this work is to model a control strategy to attain the smooth and precise switching between energy sources present in MESS. To meet the main objective of the work four hybrid controllers are modeled and implemented to the electric motor at different load conditions.

2. Representation of Proposed Model

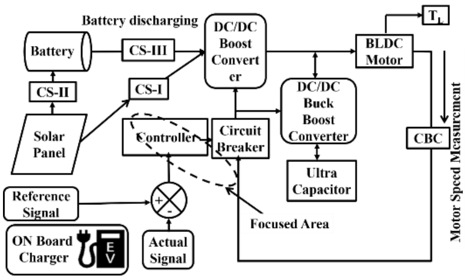

Fig. 1 Complete block diagram of the proposed model

The proposed scheme can be represented with Fig. 1 and this mainly comprising of MESS, controllers, converters and solar panels to drive. Three regulator switches are allied between the PV to the battery, PV to the unidirectional converter (UDC) and battery to UDC, these control switches are one of the deciding factors of charging and discharging periods of the battery, another one is the state of charge (SOC) of battery and output voltage level of the PV. The designed CBC and ANN/PID controller together work and generate the pulse signals to the bidirectional converter (BDC) and UDC related to the motor speed. Conventional controllers develop the control signal to the converter switches whereas the CBC controller regulates that signal related to the motor speed. The battery always gives the normal power of the motor whereas UC provides the sudden power of the motor, which means UC assists the battery during peak load conditions and starting of the motor.

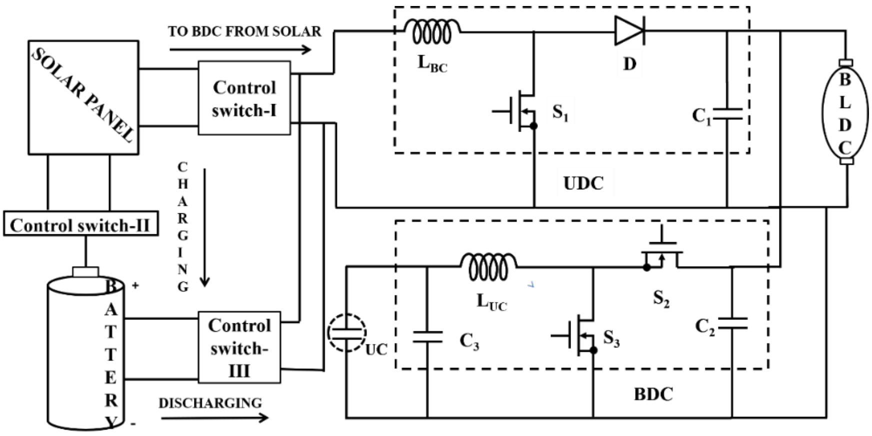

Fig. 2. MESS representation with three converter switches

Converter's main circuit has been characterized with Fig. 2; here the battery was connected at unidirectional converter end whereas UC has been connected at bidirectional converter end and two converters comprised with MOSFET switches. During boost operation of UDC, the switch S1 is in ON position whereas during boost operation of BDC switch S3 is in ON condition and during buck operation of BDC switch S2 is in ON condition. Here solar panel was used to charge the battery as well connected to the UDC directly to propel the electric drive.

3. Description of Condition-based controller (CBC)

Here CBC performances as a universal controller are generating signals to four math functions, based on electric motor speed. All math functions are programmed as per the speed of the motor and CBC having four cases of operation. This controller provides four types (U1, U2, U3, and U4) of signals by taking speed as an input. The enable and disable states of the output signals of the CBC is controlled by the speed of the motor. finally, those four signals states only control the switching signals generated by the conventional/intelligent controller which means the combination of CBC with another controller will provide the closed-loop operation of the entire system by providing soft switching between two energy sources.

4. Cases of operation of Converter Model

The overall circuit conFig.uration is divided into four cases for a better understanding of the proposed control strategy and those four cases can create related to applied load on the electric motor. Fig. 4(a) represents the case-I, in this period a huge load is applied and corresponding to that switch S3 only in enable state remain switches S2, S1 are in disable state. So, the entire power of the vehicle can be fed by the UC itself.

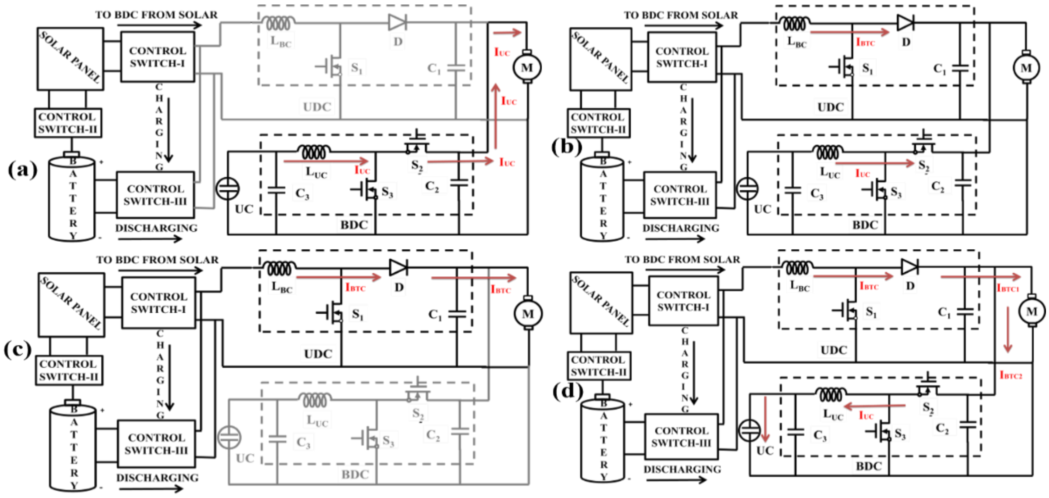

Fig. 4. MESS representation with three converter switches, (a) case-I (b) case-II (c) case-III (d) case-IV

Fig. 4(b) is stated that more than the normal load applied; at this stage, the main source and supporting source combination feeds the load. Which makes the switches S1, S3 are in enable state whereas S2 is in disable state. Case–III operation of the circuit can be represented with Fig. 4(c), in this, a normal load is applied, in this case of operation essential power by the motor can supply by the battery individually, which means switch S1 only in enable state and remain two switches S2, S3 are OFF. Finally, Fig. 4(d) can represent the no-load time on the motor during these time switches S1, S2 are in enable state and remain switch S3 is in OFF condition. In this stage, the motor needs a little bit of power that can be provided by the battery an also to charge UC.

5. Proposed Control Strategy Approach

The intended control technique is the grouping of two dissimilar controllers, in which CBC is the newly adopted controller and PI/PID/FLC/ANN are the conventional/intelligent controller. With different combinations, the precise switching is achieved related to the motor's speed. Here different combinations of hybrid controllers like CBC plus PI/PID/FLC/ANN are formed and implemented, got the unique results corresponding to the individual hybrid controller. The controller with four different hybridized combination is made up of five independent controllers. Among five controllers CBC will treat as a universal/main controller which always regulates the switching signals of converters according to the proposed technique.

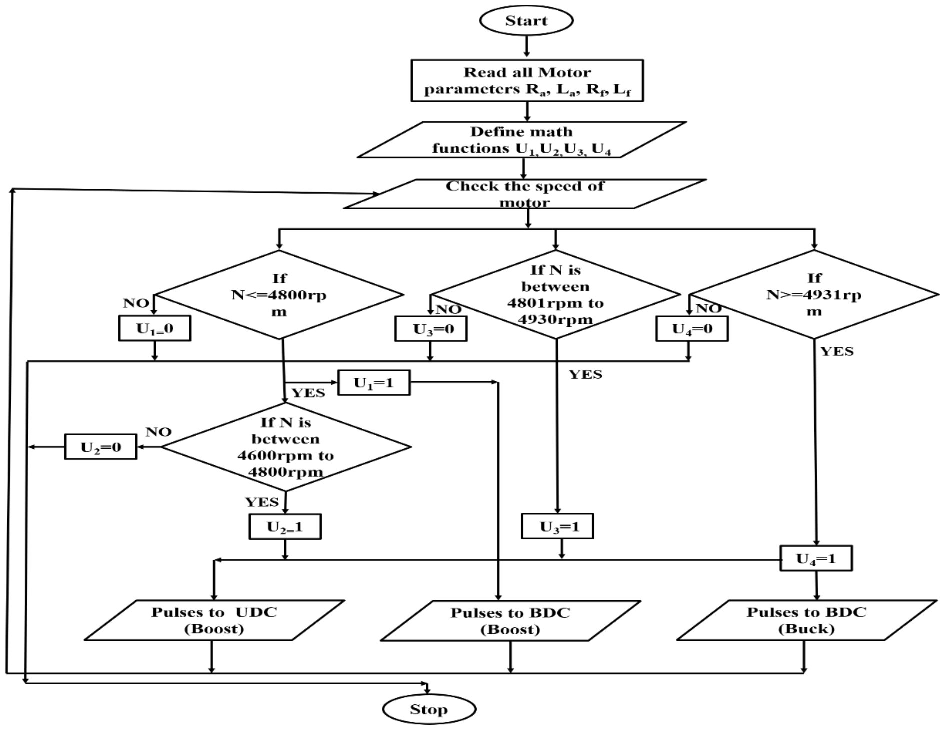

Fig. 5. Development of controlled signals to converters in a step by step representation

Fig. 5 illustrating how the controlled switching signals are producing to the converters present in the system, and which are explained point by point as bellow.

(1) When N≤4800rpm then CBC will produce output signals as one for U1. This enables the action of BDC as a boost. The complete load requirement is fulfilled by the supporting source (UC).

(2) When 4600rpm≤ N≤ 4800rpm then CBC develops output signals as “1” for U1 and U2. Which starts the operation of BDC and UDC as a boost. In this, the main source and backup source collectively sent power to the load.

(3) If 4801rpm ≤ N ≤ 4930 rpm then the CBC develops output signal as “1” for U3. Which makes that the operation of the UDC boost converter. Complete power will flow from the main source only.

(4) N≥4931rpm then CBC develops the output signal as “1” for U4. Due to which the BDC (buck) and UDC (boost) comes under working condition. In this load required power flows from the main source (battery) and the supporting sources also take power from the main source.

6. MATLAB/Simulink Results with Comparisons

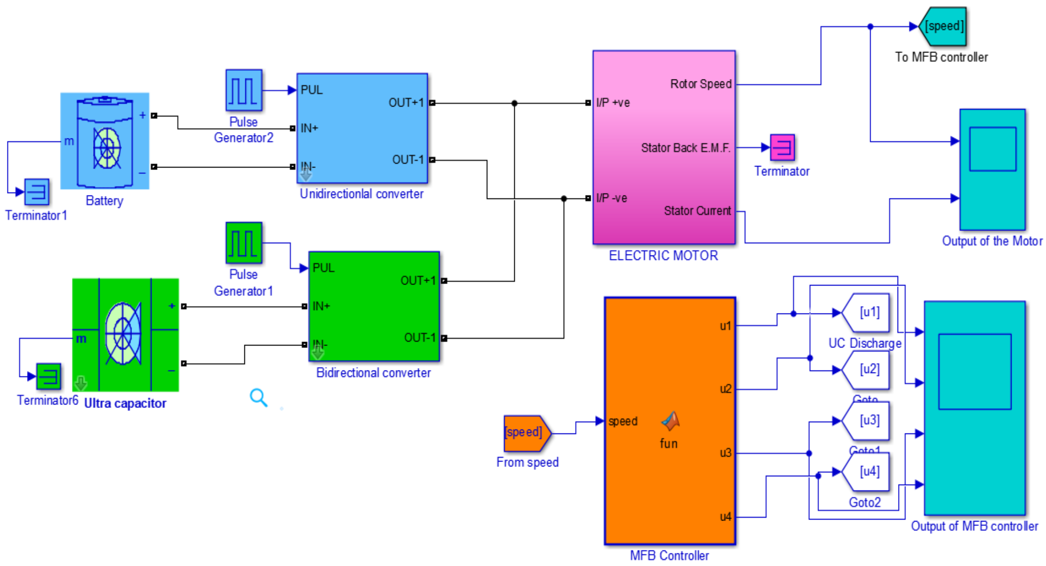

Fig. 6. MATLAB/Simulink model diagram with the proposed control strategy

The MATLAB/Simulink model with the proposed control strategy was represented in Fig. 6.

6.1 Case-I Results

Fig. 7 representing that the motor's speed corresponding to individual controllers of CBC plus ANN, CBC plus FLC, CBC plus PID, and CBC plus PI. During starting all controller responses individually different periods are taken to attain the stable state, among all the controllers CBC plus ANN is taken the minimum time (0.09 sec) and CBC plus PI is taken the maximum time (1.45 sec). And remain CBC plus FLC is taken sec time, CBC plus PID is taken a sec. At 2.5 sec a heavy load is applied due that all controllers speed dropped to less than 4600 rpm. The speed response corresponding to CBC plus ANN 0.7 sec time taken to reach a stable state, CBC plus FLC is taken 1.1 sec time and remain two controllers CBC plus PID, CBC plus PI speed responses unable to reach the stable state in specified time.

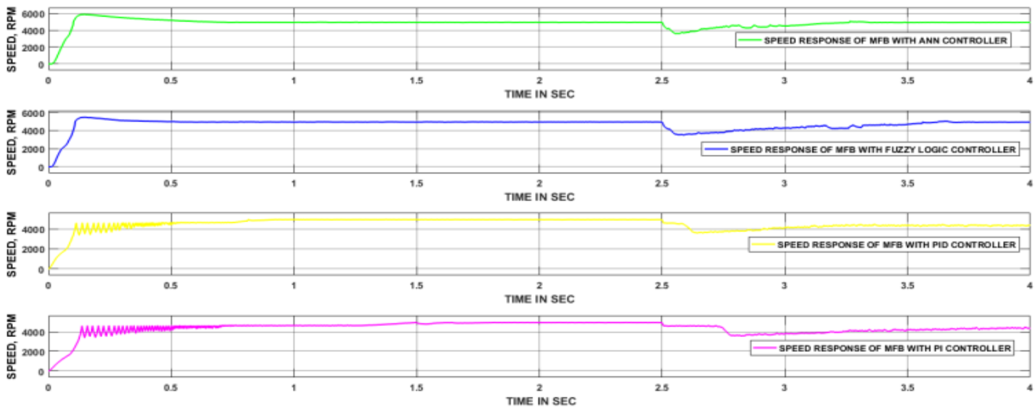

Fig. 7. Different hybrid controllers speed outcomes, case-I

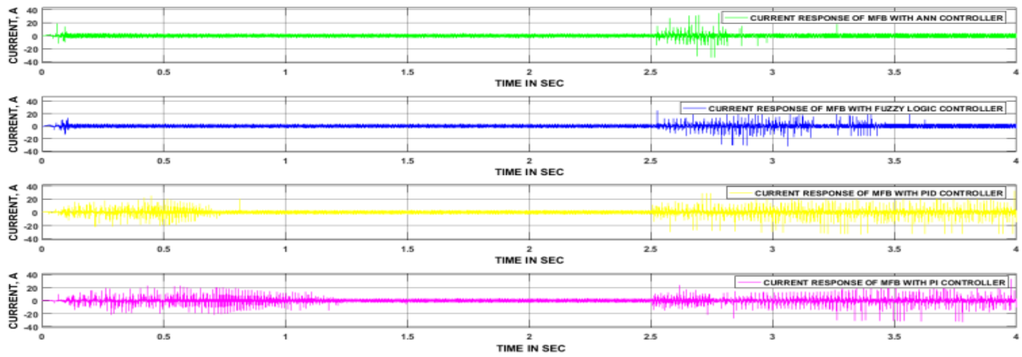

Fig. 8. Output currents of Four hybrid controllers, case-I

Fig. 8 is corresponding to the current responses of four hybrid controllers during a heavy load. At starting, the motor took extra current than rated value and after some time all controllers current response reaches a steady state. After reaching a steady-state motor draws nominal current value only until the load applied. At 2.5 sec load is applied, which leads to drawing a heavy current by the motor. After some time, CBC plus ANN, CBC plus FLC current responses reached the steady-state and remain, two controllers, CBC plus PID, CBC plus PI responses don't reach the steady-state which is clear from Fig. 8.

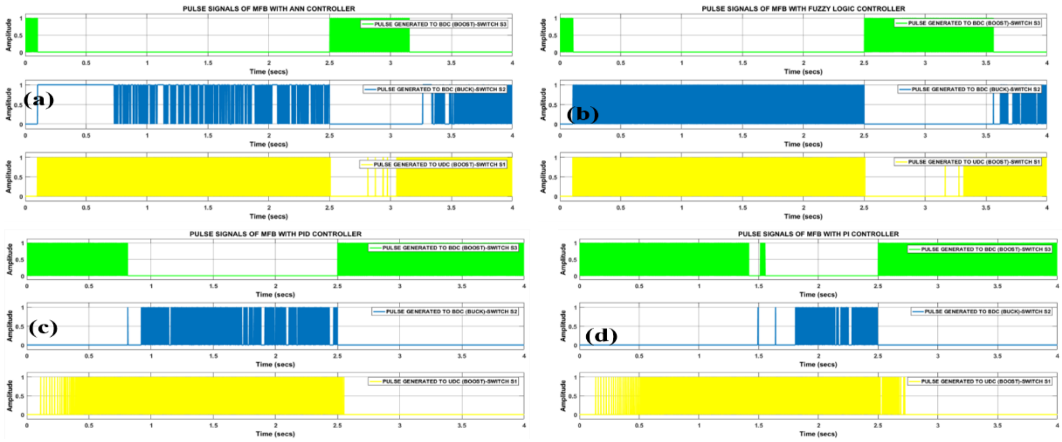

Fig. 9. Regulated switching signals of (a) CBC plus ANN controller, (b) CBC plus FLC controller, (c) CBC plus PID controller, (d) CBC plus PI controller, case-I

Fig.. 9(a) representing the regulated signals of CBC with ANN. In the initial stage of operation, the regulated pulses are developed to only BDC which initiates the BDC as boost and no pulses to UDC. After 0.1sec time main, supporting sources together provide power to the drive which begins the operation of BDC and, UDC as a boost. After some time, the main source itself gives the total power to the load which starts the operation of UDC (boost) until the load is applied. The load is applied at 2.5 sec, which initiates the operation of BDC (boost). Again, motor response reaches the stable state within 0.7 sec with the controller action which starts the UDC operation (boost) and BDC (buck), which will continue till the load applied. Fig.. 9(b) shows the signals of CBC with FLC, at 2.5-sec load, is applied, which initiates the operation of BDC (boost). Again, motor response reaches the stable state within 1.1 sec with the controller action which starts the UDC operation (boost) and BDC (buck), which will continue till the load is applied. Fig. 9(c) &9(d) shows the pulses of CBC with PID, PI and at 2.5-sec load is applied, which initiates the operation of BDC (boost). The motor response has not attained a stable state due to a heavy load.

6.2 Case-II Results

Fig.. 10 representing the speed responses of the motor during slightly more than the rated load. At 2.5 sec load is applied on the due that all controllers speed responses dropped between 4600 to 4800 rpm. The speed response corresponding to CBC plus ANN took 0.2 sec to attain normal response, CBC plus FLC took 0.25 sec time and remain, two controllers, CBC plus PID, CBC plus PI speed responses took 0.4 sec and 0.3 sec time to obtain the original response.

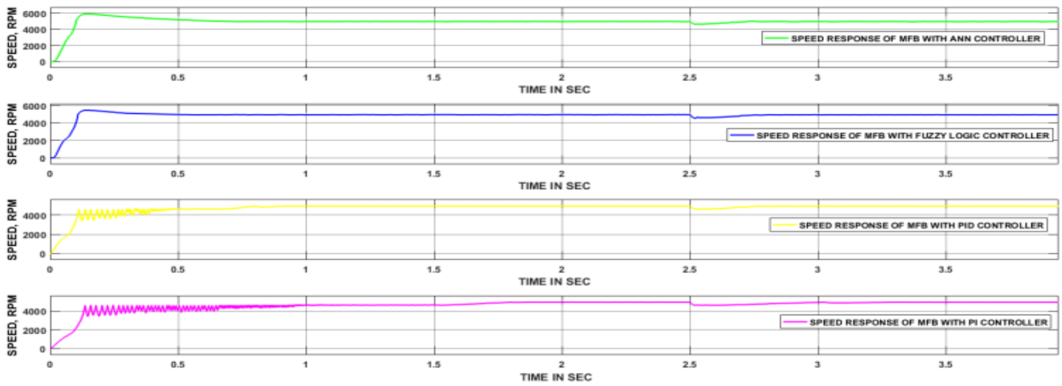

Fig. 10. Different hybrid controllers speed outcomes, case-II

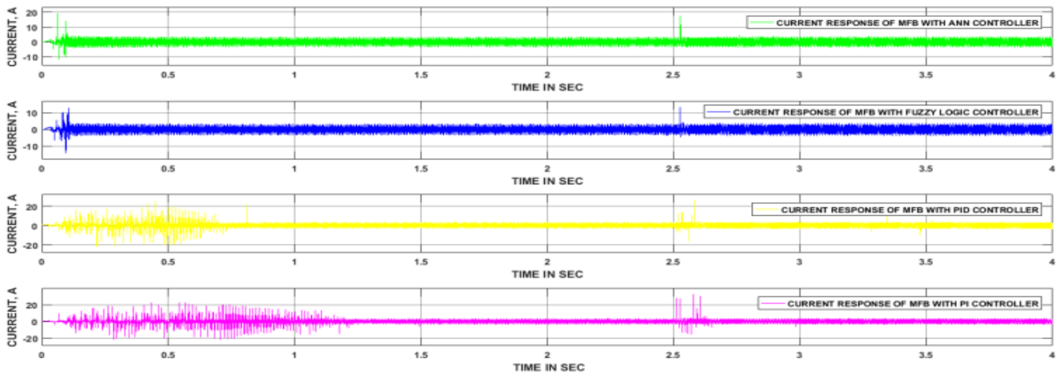

Fig. 11. Output currents of Four hybrid controllers, case-II

The desired load is applied at 2.5 sec, which leads to drawing slightly more than rated current by an electric motor. After some time, CBC plus ANN, CBC plus FLC, CBC plus PID, and CBC plus PI current responses reached the steady-state by their periods which is clear from Fig. 11.

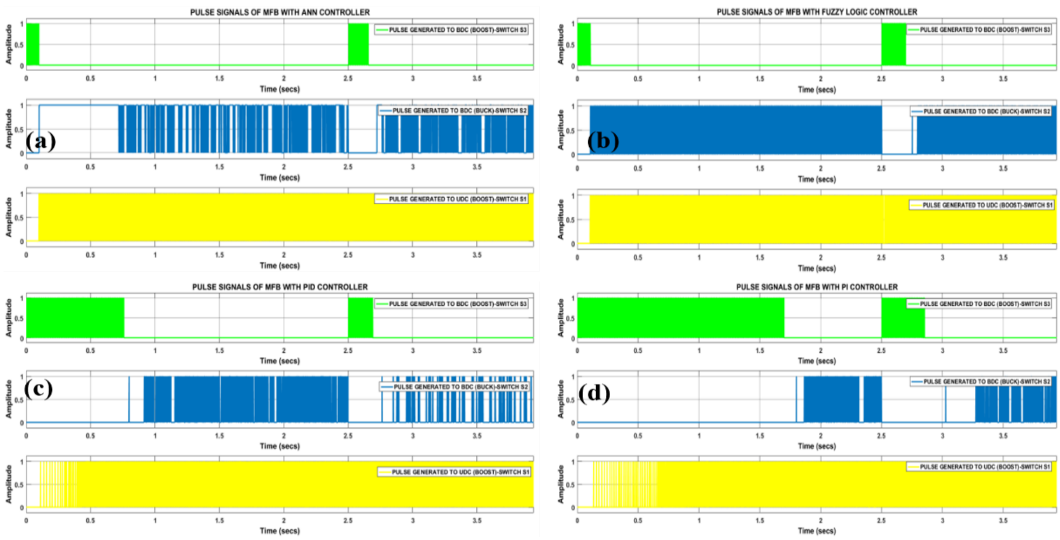

Fig. 12. Regulated switching signals of (a) CBC plus ANN controller, (b) CBC plus FLC controller, (c) CBC plus PID controller, (d) CBC plus PI controller, case-II

6.3 Case-III Results

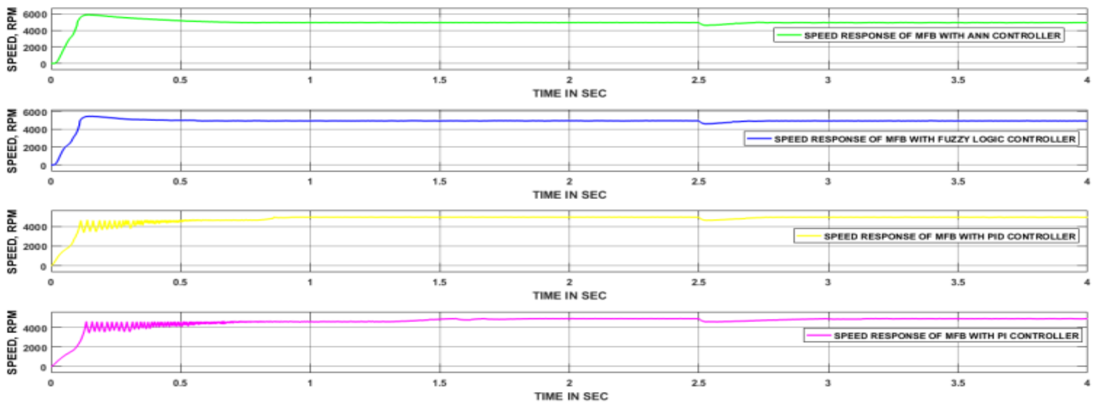

Fig. 13. Different hybrid controllers speed outcomes, case-III

Fig. 13 illustrating the, after applying the rated load at 2.5 sec, all controllers speed responses sustained between 4801 rpm to 4930 rpm. The speed response corresponding to CBC plus ANN 0.1sec time taken to reach steady-state, CBC plus FLC is taken 0.12 sec time and remain controllers CBC plus PID, CBC plus PI speed responses 0.15 sec and 0.3 sec time taken to reach the original response.

The corresponding load is applied at 2.5 sec, which leads to drawn rated current by an electric motor. After some time, CBC plus ANN, CBC plus FLC, CBC plus PID, and CBC plus PI current responses reached the steady-state (with each controller individual time) which is clear from Fig. 14.

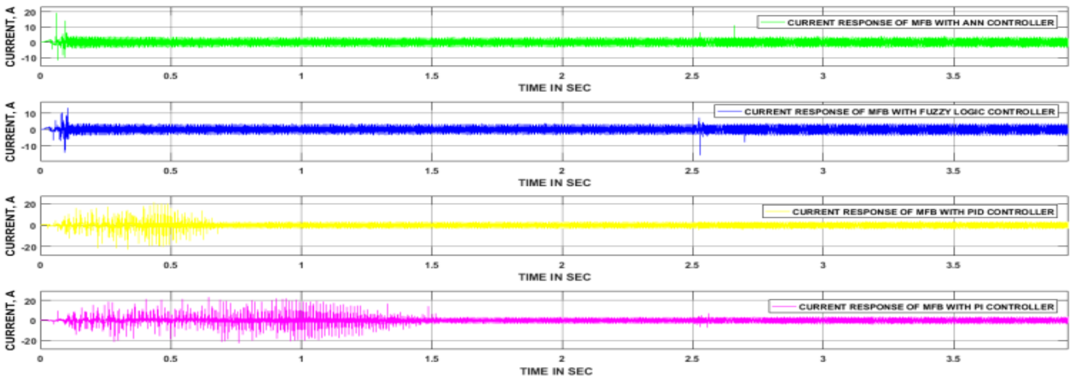

Fig. 14. Output currents of Four hybrid controllers, case-III

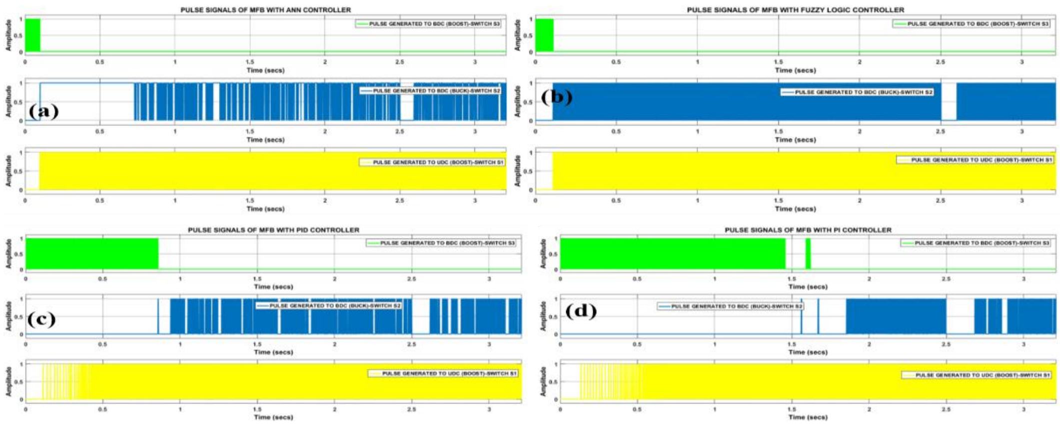

Fig. 15. Regulated switching signals of (a) CBC plus ANN controller, (b) CBC plus FLC controller, (c) CBC plus PID controller, (d) CBC plus PI controller, case-III

6.4 Case-IV Results

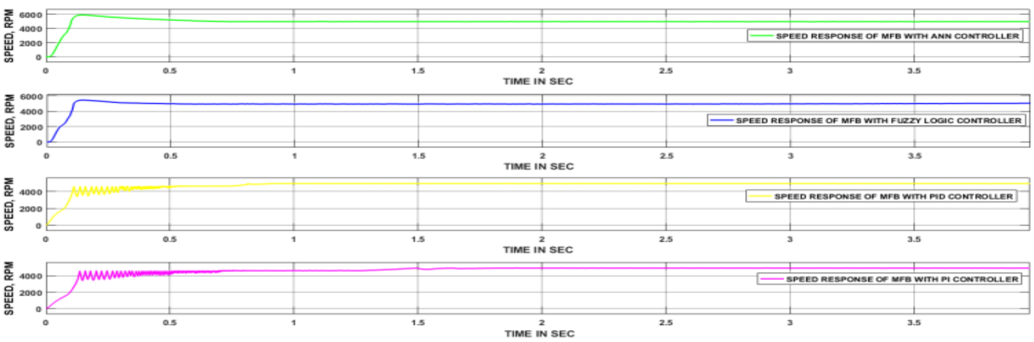

Fig. 16. Different hybrid controllers speed outcomes, case-IV

Fig. 16 shows that the EV is running under load free, so no speed changes observed once the motor reaches the steady-state condition.

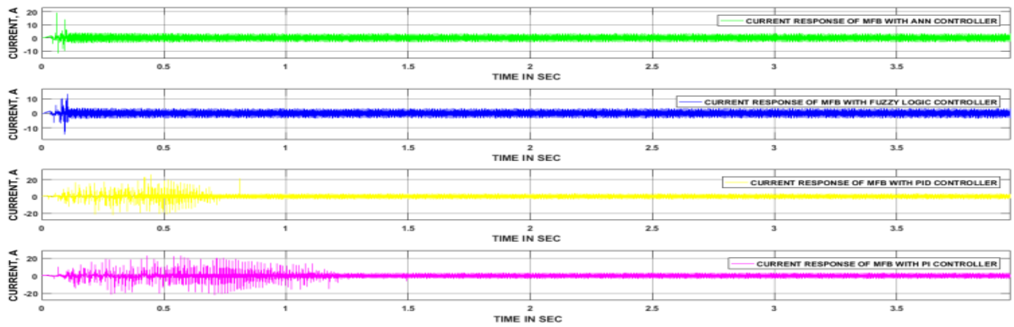

Fig. 17. Output currents of Four hybrid controllers, case-IV

In case-IV operation, no-load applied which means no current variations find in Fig. 17 after reaching the steady-state.

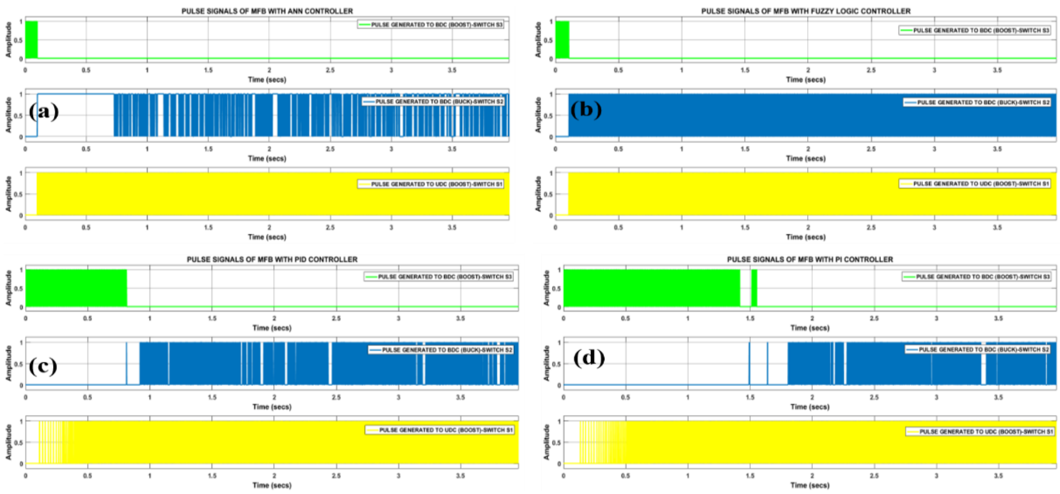

Fig. 18. Regulated switching signals of (a) CBC plus ANN controller, (b) CBC plus FLC controller, (c) CBC plus PID controller, (d) CBC plus PI controller, case-IV

Table 1 indicates, during case-I CBC plus ANN and CBC plus FLC are 0.7 sec and 1.1sec time taken to reach the stable state while CBC plus PID and CBC plus PI unable to reach the stable state within a specified time. In case-II, CBC plus ANN/FLC/PID/PI controllers are 0.2, 0.25, 0.3 and 0.4 sec time taken to reach a steady state. During case-III operation the designed controllers CBC plus ANN/FLC/PID/PI are taken 0.1, 0.12, 0.15 and 0.3sec of time to attain a stable state. Finally, the motor is running without a load in case-IV operation.

Table 1

Performance analysis of four hybrid controllers related to the case of operation

Controller	Time to attain original response of the wave after applying various loads(sec)			
	Case-I	Case-II	Case-III	Case-IV
CBC plus ANN	0.7	0.2	0.1	No load state
CBC plus Fuzzy	1.1	0.25	0.12	No load state
CBC plus PID	Not reached stable state	0.3	0.15	No load state
CBC plus PI	Not reached stable state	0.4	0.3	No load state

Table 2

Comparative study of four hybrid controllers based on different time domain specification

Parameter	**CBC with ANN**	**CBC with FLC**	**CBC with PID**	**CBC with PI**
Delay time (sec)	0.07	0.09	0.1	0.15
Rise time (sec)	0.9	0.1	0.7	1.4 s
Peak time (sec)	0.15	0.15	0.8	1.5
Settling time (sec)	0.9	0.1	0.85	1.45
Maximum peak overshoot (%)	20	10	2	2

Table 2 representing the performance study among four hybrid controllers based on the time domain specifications. This analysis is useful to know the suitable controller for EV application according to the proposed control technique.

7. Conclusions

By combining the designed CBC with conventional controllers formed an innovative control approach that is useful during swapping of energy sources present in MESS. CBC controller played a dynamic role during the transition period by regulating the switching signals produced by the other controllers like PI, PID, FLC, and ANN. Based on the projected control strategy four separate hybrid controllers (CBC plus PI, CBC plus PID, CBC plus FLC, and CBC plus ANN) are implemented to the main EV model and attain satisfactory results from all controllers. All hybrid controller’s performance is compared based on the delay time, rise time, peak time, settling time and maximum peak overshoot and presented in the conclusion section. Among all the controller's performance, CBC plus ANN is given an improved performance during switching of battery and UC as per the electric vehicle requirement. For all controller’s case, in case-I, controlled signals are produced to only BDC (boost) and no signals to UDC.

During case-II, switching signals are produced to UDC (boost) and BDC (boost). In case-III, the switching signals are produced to only UDC (boost) and no signals to BDC. In case-IV, the EV is running under normal mode of operation. In all the above cases, pulse changes happen because of hybrid controllers' actions only.

R E F E R E N C E S

[1]. *Akar, Furkan, Yakup Tavlasoglu, and Bulent Vural,* "An energy management strategy for a concept battery/ultracapacitor electric vehicle with improved battery life." IEEE Transactions on Transportation Electrification **Vol.3**, no. 1, 2016, pp. 191-200.

[2]. *Duan, C., Wang, C., Li, Z., Chen, J., Wang, S., Snyder, A., & Jiang, C,* "A Solar Power Assisted Battery Balancing System for Electric Vehicles", IEEE Transactions on Transportation Electrification, 2018

[3]. *Liu, N., Chen, Q., Lu, X., Liu, J., & Zhang, J,* "A Charging Strategy for PV-Based Battery Switch Stations Considering Service Availability and Self-Consumption of PV Energy", IEEE Trans. Industrial Electronics, **Vol.162**, no. 8, 2015, pp. 4878-4889.

[4]. *Hu, S., Liang, Z., & He, X,* "Ultracapacitor-battery hybrid energy storage system based on the asymmetric bidirectional Z-source topology for EV", IEEE Transactions on Power Electronics, **Vol.31**, no. 11, 2016, pp.7489-7498.

[5]. *Ghiassi-Farrokhfal, Y., Kazhamiaka, F., Rosenberg, C., & Keshav, S,* "Optimal design of solar PV farms with storage" IEEE Transactions on Sustainable Energy, **Vol.6**, no. 4, 2015, pp. 1586-1593.

[6]. *Keil, P., Englberger, M., & Jossen, A,* "Hybrid energy storage systems for electric vehicles: An experimental analysis of performance improvements at subzero temperatures" IEEE Transactions on Vehicular Technology, **Vol.65**, no. 3, 2016, pp.998-1006.

[7]. *Li, J., Zhang, M., Yang, Q., Zhang, Z., & Yuan, W,* "SMES/battery hybrid energy storage system for electric buses", IEEE Transactions on Applied Superconductivity, **Vol.26**, no. 4, 2016, pp.1-5.

[8]. *Shen, J., & Khaligh, A,* "Design and real-time controller implementation for a battery-ultracapacitor hybrid energy storage system" IEEE Transactions on Industrial Informatics, **Vol.12**, no. 5, 2016, pp.1910-1918.

[9]. *Trovao, J. P., Roux, M. A., Ménard, É., & Dubois, M. R,* "Energy-and power-split management of dual energy storage system for a three-wheel electric vehicle" IEEE Trans. Veh. Technol, **Vol.66**, no. 7, 2017, pp.5540-5550.

[10]. *Chaudhari, K., Ukil, A., Kumar, K. N., Manandhar, U., & Kollimalla, S. K*, "Hybrid optimization for the economic deployment of ESS in PV-integrated EV charging stations", IEEE Transactions on Industrial Informatics, **Vol.14**, no. 1, 2018, pp.106-116.

[11]. *Mesbahi, T., Rizoug, N., Bartholomeüs, P., Sadoun, R., Khenfri, F., & Le Moigne, P,* (2017). "Optimal Energy Management for a Li-Ion Battery/Supercapacitor Hybrid Energy Storage System Based on a Particle Swarm Optimization Incorporating Nelder–Mead Simplex Approach" IEEE Transactions on Intelligent Vehicles, **Vol.2**, no. 2, 2017, pp. 99-110.

[12]. *Lu, X., Chen, Y., Fu, M., & Wang, H, "*Multi-Objective Optimization-Based Real-Time Control Strategy for Battery/Ultracapacitor Hybrid Energy Management Systems", IEEE Access, **Vol.115**, no. 7, 2019, pp.11640-11650.